

Table 1: Time intervals, Initial and boundary conditions used in the modeling of the foundation.

Interval and Boundary Conditions	Interval	Boundary Conditions	
	1 Foundation load 0-4 [days]	<i>Lower boundary(1):</i> $u_y = 0$ $p_l = 0.15 \text{ MPa}$ $T = 15.4 \text{ }^\circ\text{C}$	<i>On top of foundation:</i> 1a) $\dot{u}_y = 0.0048 \text{ mm/min}$ up to q_{serv} . 1b) <i>On free soil surface:</i> Atmospheric load (root_atm.dat)
	2 Atmospheric load only 4-50 [days]	<i>Lower boundary(1):</i> $u_y = 0$ $p_l = 0.15 \text{ MPa}$ $T = 15.4 \text{ }^\circ\text{C}$	<i>On free soil surface:</i> Atmospheric load (root_atm.dat)
	3 Atmospheric load only 50-350 [days]	<i>Lower boundary(1):</i> $u_y = 0$ $p_l = 0.13 \text{ MPa}$ $T = 15.4 \text{ }^\circ\text{C}$	<i>On free soil surface:</i> Atmospheric load (root_atm.dat)

Table 2: Load and model configuration used in the modeling of the foundation.

Load Configuration	
Model Configuration at prototype (field) scale	<p>Finite element mesh 450 elements</p> <p>axisymmetric axis</p> <p>u_y (vert. displacement) = 0 p_l (liq. pressure) = <i>prescribed</i> T (temperature) = <i>prescribed</i></p> <p>u_x (horiz. displacement) = 0 q_l (liq. flux) = 0 $i_{e,r}$ (heat flux) = 0</p>

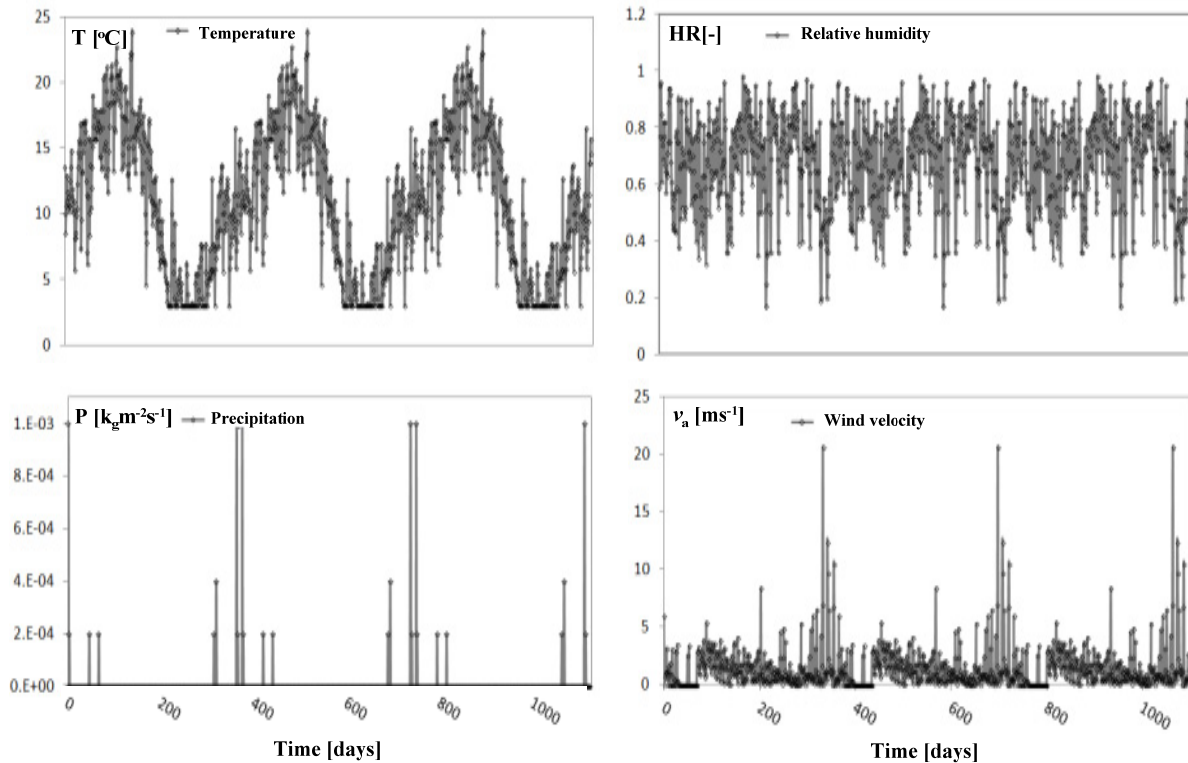


Figure 2. Atmospheric load applied at the soil surface of the silty column.

Material parameters

As for the mechanical model, a hyperplastic constitutive law has been used to model the silty material (Samat 2016). In hyperplasticity two energy functions must be defined to fully derive the constitutive law. Those energy functions are the energy potential g_s and the dissipation function d_s (alternatively the yield function f^y). Both functions are sensitive to suction and temperature. The former is taken into account at g_s by using a skeleton effective stress $p' = p'' + S_1 s$ often adopted in unsaturated soil mechanics modeling and at f^y by affecting the mean yield stress due to the bonding effect that water meniscus produces between soil particles in the unsaturated soil, thus expanding the elastic domain of response. The temperature affects the energy function so that the resulting thermal strains turns out pressure dependent, while the yield function is affected in its mean yield stress so that any increase of temperature leads to a shrinkage of the elastic domain of response, (Samat 2016).

Both functions written in terms of triaxial invariants (the mean skeleton stress p' and the deviatoric stress q) and environmental variables (suction s and temperature T) are presented in Table 3 together with the material parameters used for the mechanical model.

Table 3: Mechanical material parameters and energy functions

MECHANICAL DATA	
a) Gibbs potential:	
$g_s = \frac{(1 - \beta_s(\alpha_T))}{p_0^{1-n} \cdot k(1-n)(2-n)} \cdot \left(p'^2 + \frac{k(1-n)}{3q} q^2 \right)^{\frac{2-n}{2}} - \frac{p'(1 - \beta_s(\alpha_T))}{k(1-n)} - (p'\alpha_p + q\alpha_q)$	
with	
$\beta_s(\alpha_T) = k(1-n) \frac{\alpha_T}{3} \cdot (T - T_o) \left(1 - \frac{T-T_o}{2T_m} \right)$ (Samat 2016)	
b) Yield function:	
$f^y = p'^2 + \frac{q^2}{M^2 B(\epsilon)^2} - w(s)^2 \cdot \left(\frac{p_o^*}{2} \right)^{2b(s)} \left(1 - c_T \ln \left(\frac{T}{T_o} \right) \right)$	
$B = \epsilon + (1 - \epsilon) \frac{p}{p_o}$ Collins & Kelly (2002) and $w(s)$ and $b(s)$ are suction dependent funcs. Samat (2016) M is the slope of the CSL in the p' - q plane.	
Elastic Parameters	
κ slope isotropic compression line in v - $\ln p'$ plane	0.005
ν Poisson's coefficient	0.3
n amount of non-linearity	0.9
Thermal Parameters	
$\alpha_T \left[\frac{1}{^\circ\text{C}} \right]$ linear thermal dilatancy	3e-6
T_o [$^\circ\text{C}$] reference temperature	$\equiv T_{initial}$ at the corresponding point
Plastic Parameters	
p_o^* [MPa] saturated mean yield stress	0.07
ϕ [$^\circ$] inner friction angle	31
N specific volume at $p'=1$ MPa	1.65
λ slope of saturated normal compression line	0.07
a, b shape parameters of the LC yield surface	0.0048, 3.4
$c_T \left[\frac{1}{^\circ\text{C}} \right]$ thermal degradation parameter for p_o	2.46e-3
η [-] viscosity	1e-3
Shape Parameters	
ϵ [-] shape param. for f^y in the p' - q plane	0.5
Integration Parameters	
Algorithm index	3 (interior point algorithm)
Newton tolerance	1E-6
Line_search param. 1	1E-2
Line_search param. 2	0.1
Max. iter. barrier	1
Max. iter. Newton	30
Max. Line_search iter.	5

Table 4 summarizes the material parameters of the hydraulic and thermal laws. They complete the set of material parameters of the proposed climate model.

Table 4: Parameters of the hydraulic and thermal laws. Parameters of the solid phase

HYDRAULIC- THERMAL - PHASE DATA		
Parameter	Value	Law
Retention Curve (simpl. van Genuchten)		
p_0 [MPa] air entry value parameter	0.013	$S_r = \left(1 + \frac{s}{p_0}\right)^{-\lambda}$
λ shape parameter	0.52	
S_{r1} residual saturation	0.38	
Intrinsic Permeability (Kozeny's model)		
k_{ii} [m ²] intrinsic permeability	2.85E-14	$k = k_0 \frac{\phi^3 (1 - \phi_0)^2}{(1 - \phi)^2 \phi_0^3}$
ϕ_0 reference porosity	0.4583	
Liquid Phase Rel. Permeability (van Genuchten law)		
λ shape parameter	0.52	$k_{r1} = \sqrt{S_r} \left(1 + \frac{s}{p_0}\right)^{-\lambda}$
Diffusive flux of Vapor (Fick's law)		
D [m ² Pa/sKn] diffusivity	5.9E-10	$i_a^i = -(\tau\phi\rho_a S_a D(T)I)\nabla\omega_a^i$
N	2.3	
τ_0 tortuosity	1.0	
Conductive Flux of Heat (Fourier's law)		
λ_{dry} [WmK ⁻¹] thermal cond. dry medium	1.48	$i_c = -\lambda\nabla T$
λ_{sat} [WmK ⁻¹] thermal cond. saturated medium	2.0	
Solid Phase (Density)		
C_s [Jkg ⁻¹ K ⁻¹] specific heat	1000	
α_T [1/°C] thermal dilatancy	3E-6	
ρ_s [kgm ⁻³] solid grains density	2700	

Model results

Figure 3 shows a general overview of the obtained results contrasted with the input records of wind velocity and temperature. First row (a) corresponds to the evolution of wind velocity, the second row (b) is the evolution of the atmospheric temperature at the column surface, the third row (c) is the computed evolution of temperature at a point below the foundation, then the fourth row (d) corresponds to the computed evolution of the degree of saturation, fifth row (e) shows the computed evolution of the absolute vertical displacement and finally row (f) corresponds to the obtained evolution of differential vertical displacement observed between the footing center and the footing edge.

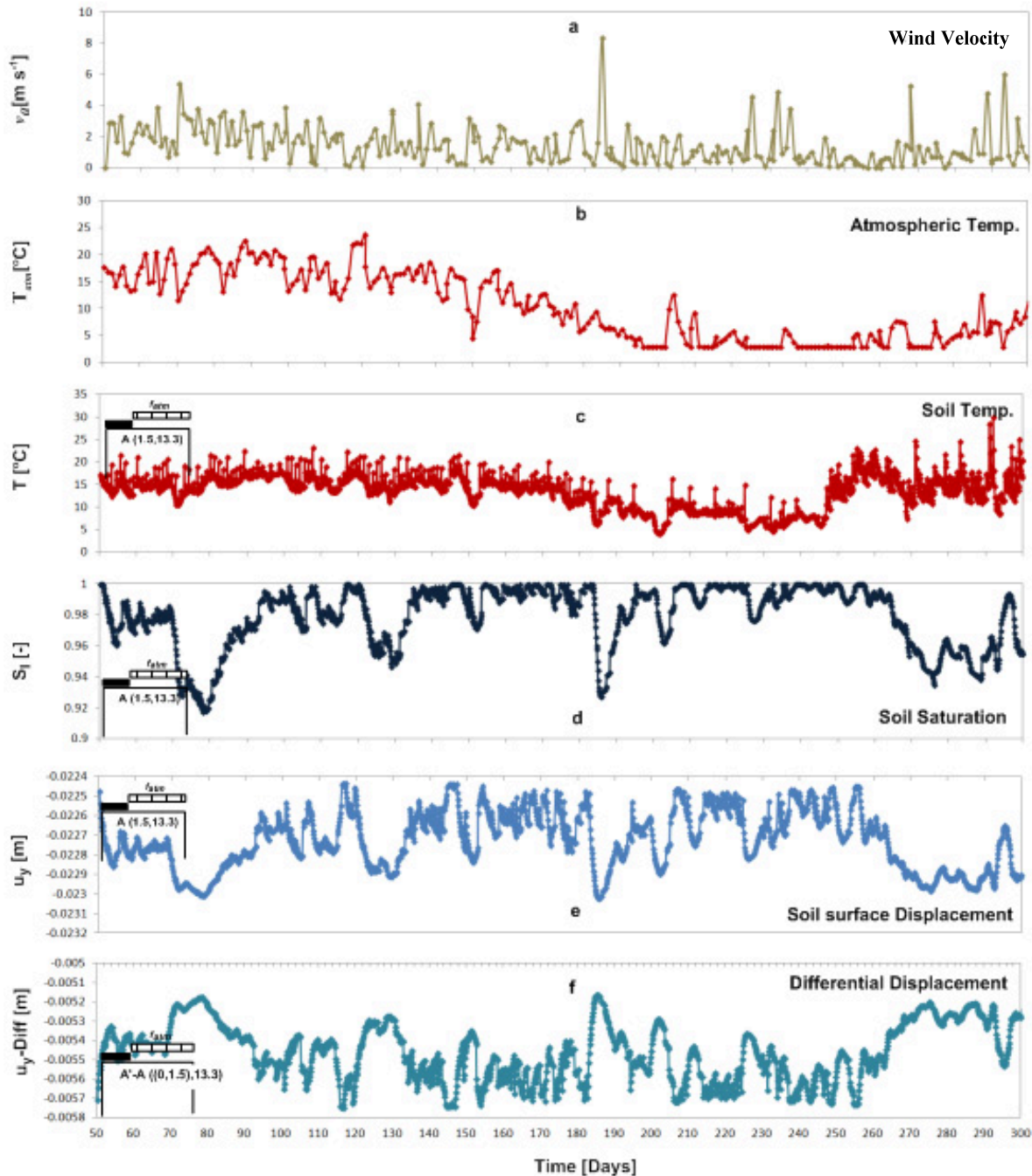


Figure 3. Overall view of the modeled case. (a) and (b) Records of wind velocity and atmospheric temperature applied at the column surface, (c) and (d) Computed evolutions of soil temperature and degree of saturation at the footing edge, (e) Evolution of vertical displacements at the upper soil layer of the silty column and (f) Evolution of vertical differential displacements observed between the footing center and the footing edge.

The existing differences between the atmospheric temperature and the computed temperature at the column surface are due to the applied radiation which contributes to the total input heat flux

(Eq. 3). Variation of the degree of saturation shows a monthly character of dry periods followed by wet periods. As a result of the temperature and degree of saturation, the maximum amplitude of soil displacement is 6 mm. This amplitude presents a typical variation in periods of several days. The relative settlement between the center and the edge of the foundation is 5.8 mm which gives an angular variation of $3E-4$.

Figure 4 presents the stress paths and yield surfaces obtained at different times during the atmospheric action.

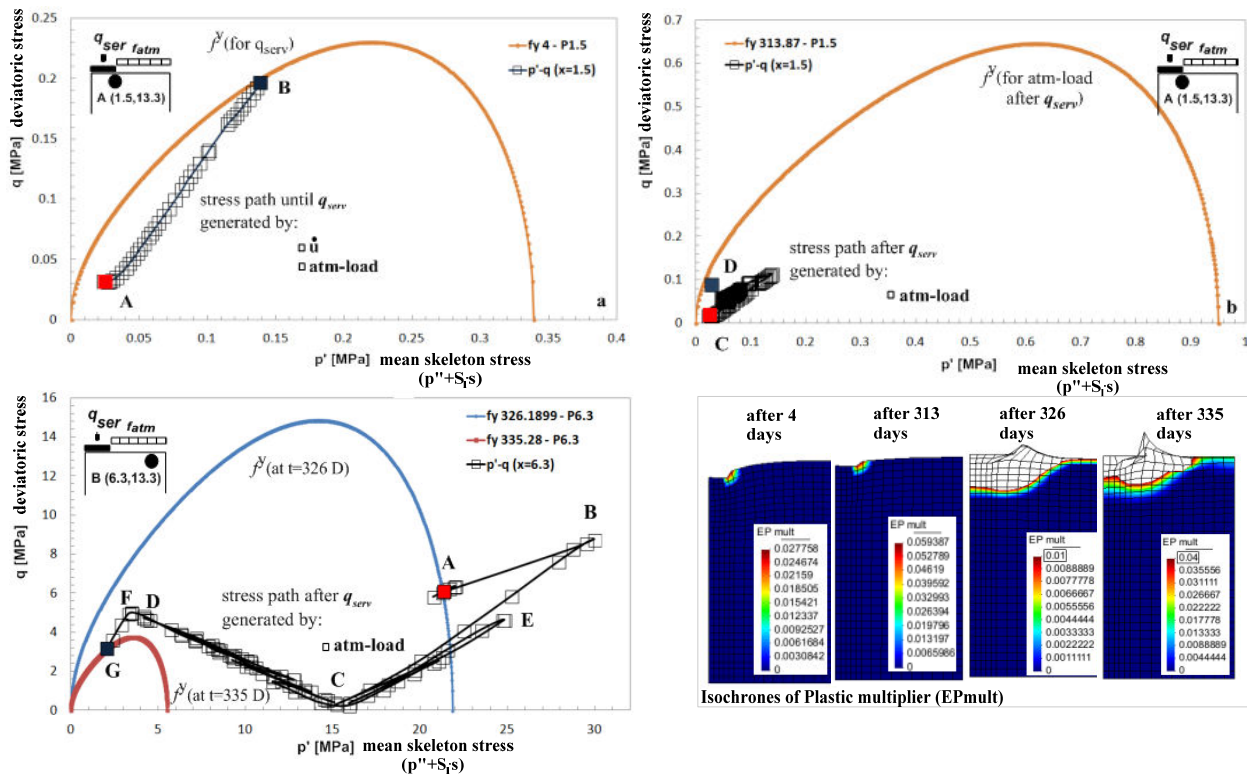


Figure 4. Stress paths and yield surfaces at times: (a) of foundation's load at service value and (b) after 313 days, (c) between 326-335 days after the atmospheric load onset and (d) isochrones of the plastic multiplier.

A remarkable effect of drying by a considerable increase of sun radiation is observed at day 335 which produces a softening of the material surrounding the foundation and an important uplift of the soil next to the foundation edge.

CONCLUSIONS AND FINAL REMARKS

The proposed climatic model for geotechnical applications considers the flows of water, air and energy of the atmosphere in its lowest layer in contact with the ground surface. Each component of these flows has its counterpart of the same phase (liquid-gas) and the same species (water-air) in the porous medium. This fact confers the model with a complete consistency.

The strong THM coupling of the problem requires robust mechanical constitutive models to be able to provide a proper response in terms of displacement, stress, and strain to the action of the climate on the ground.

The proposed model has been used to study the response of a shallow foundation resting on a partially saturated homogeneous silt layer. The necessary robustness of the mechanical model has been achieved by formulating the model within the thermodynamic framework of hyperplasticity. To do this, two scalar energy functions are proposed, which are sensitive to the environmental actions of suction and temperature.

Under the action of an atmospheric load typical for the central Catalonia the study of the shallow foundation has shown important results of the foundation response. As result of temperature and suction variations, the foundation has experienced a maximum displacement amplitude of 6 mm. This amplitude presents a typical variation in periods of several days. The relative settlement between the center and the edge of the foundation is 5.8 mm which resulted in an angular variation of $3E-4$. A significant event of atmospheric radiation, in the final period of the atmospheric load, produces a strong drying process of the soil which results in large vertical displacements of about 3cm at footing edge.

Having a climate model for geotechnical applications is undoubtedly relevant in the design and dimensioning stages of geotechnical structures. Events with appropriate recurrence periods allow to study extreme situations for such structures.

REFERENCES

- Carreras, J., Alfageme, H., Galarza, G., Medina, A., & Andres, M. (1991). Estudio de la infiltración através de la cobertera de la F.U.A. Barcelona-España: Centro Internacional de Metodos Numericos en Ingeniería.
- Collins, I., & Kelly, P. (2002). A thermomechanical analysis of a family of soil models. *Géotechnique* 52, No 7 , 507-518.
- Gens, A. (2010). Soil-environment interactions in geotechnical engineering. *Geotechnique* 60, No 1 , 3-74.
- Noilhan, J., & Mahfouf, J. (1996). The ISBA land surface parameterization scheme. *Global and planetary change*, 13 , 145-159.
- Samat, S. (2016). Thermomechanical modeling of ground response under environmental actions. Barcelona: PhD. Thesis-BarcelonaTECH.

THM Evolution of Bentonite in China-Mock-Up Test for High-Level Radioactive Waste Disposal in China

Y. M. Liu, Ph.D.¹; and S. F. Cao, Ph.D.²

¹CNNC Key Laboratory on Geological Disposal of High-level Radioactive Waste, Beijing Research Institute of Uranium Geology, P.O. Box 9818, N.10, Xiao-Guan-Dong-Li, Anwai, Beijing, R.P. China. E-mail: liuyuemiao@163.com

²CNNC Key Laboratory on Geological Disposal of High-level Radioactive Waste, Beijing Research Institute of Uranium Geology, P.O. Box 9818, N.10, Xiao-Guan-Dong-Li, Anwai, Beijing, R.P. China. E-mail: csf831016@163.com

Abstract

Based on the preliminary concept of the high-level radioactive waste (HLW) repository in China, a large scale China-mock-up test, intended to study the thermo-hydro-mechanical-chemical (THMC) behavior of GMZ bentonite was built. The temperature of the heater was increased progressively to 90°C which is the maximum temperature expected on the canister surface in China. The hydration with the underground water from the host granite rock in Beishan site was initially controlled by a water injection rate and then controlled by a given variation of water pressure from 0.2 to 0.5 MPa. Temperature, relative humidity (RH), and stress in the compacted bentonite were recorded continuously since January 1, 2011. The temperature of compacted bentonite increased quickly at the beginning stage and then increased slowly. RH indicated that the compacted bentonite became saturated progressively. The experimental results evaluated the THMC processes occurring in the compacted bentonite during the early stage of HLW disposal and could provide a reliable database for the design of HLW repository.

INTRODUCTION

According to the research and development guide of HLW disposal in China, the spent fuel from nuclear power plants will be reprocessed first, followed by vitrification and final disposal. The preliminary concept for China's HLW repository will be a shaft-tunnel model with a multi-barrier system, located in saturated zones in granite (Wang 2006). GMZ bentonite is currently considered as the candidate buffer and backfill material for the HLW disposal in China. Comprehensive studies have been conducted on the GMZ bentonite (Liu 2003, 2007; Ye 2009; Cui 2011). Based on the

preliminary concept of HLW repository in China, the large scale China-Mock-up test, intended to study the THMC behavior of GMZ bentonite under relevant repository condition, was built in the laboratory of Beijing Research Institute of Uranium Geology (BRIUG) (Liu 2013). The experiment could demonstrate the technical feasibility, to evaluate THMC processes taking place within the compacted bentonite during the early phase of HLW disposal and to provide a reliable database for numerical modeling and further investigations.

To understand the complex behavior of buffer/backfill material subjected to thermo-hydro-mechanical (THM) processes, an increasing interest has been shown by the international community. As a result, advanced experimental facilities both in situ and in laboratory have been developed during the last decades. In particular, it is worth mentioning the Long Term Experiment of Buffer Material (LOT) series at the Äspö HRL in Sweden (Karlund 2000), FEBEX experiment in Spain and Switzerland (Martin 2005; Villar 2005), OPHÉLIE and PRACLAY heater experiments in Belgium (Romero 2006; Li 2010) and Mock-Up-CZ experiment in Czech Republic (Pacovsky 2007). The experimental results obtained from these large-scale experiments provide important references to investigate the behavior of bentonite under simulative HLW disposal conditions.

In this paper, the experimental data acquired in China-Mock-Up since 1st January 2011 are presented and analyzed, including the variation of temperature, RH and the total stress.

DESCRIPTION OF THE EXPERIMENTAL INFRASTRUCTURE

The main components of the China-Mock-up experiment are designed as follows (Figure 1): a steel tank (diameter 900mm × high 2200mm) to simulate the vertical gallery; a central electrical heater by carbon steel which substitute the waste canister (diameter 300mm × high 1600mm, weight:1 ton) with a temperature control system; a hydration system to simulate the water penetration; the engineered barrier composed of the compacted GMZ bentonite surrounding the heater; sensors; gas measurement and collection system; and a Data Acquisition System (DAS).

GMZ bentonite from underground was dried to water content of 8%, and then crushed to particle diameter size 74 μm and 178 μm which were named GMZ-001 and GMZ-06 separately. According to the X-diffraction analysis, the mineral composition of GMZ bentonite is dominated by montmorillonite, with variable quantities of quartz, cristobalite, feldspar, calcite and kaolinite (Table 1). A computer-controlled triaxial experiment machine in combination with specially designed steel molds was used to compact the GMZ-06 powders into blocks with dry density 1.71g/cm^3 . The bentonite blocks compacted by GMZ-001 with dry density 1.93g/cm^3 were crushed into pellets with an average dry density 1.3g/cm^3 in different grain sizes which was filled the space

between the bentonite blocks and the heater/steel tank walls in the China-Mock-Up. The total mass of bentonite used in the experiment is about 2.1 tons with an average dry density 1.6 g/cm^3 .

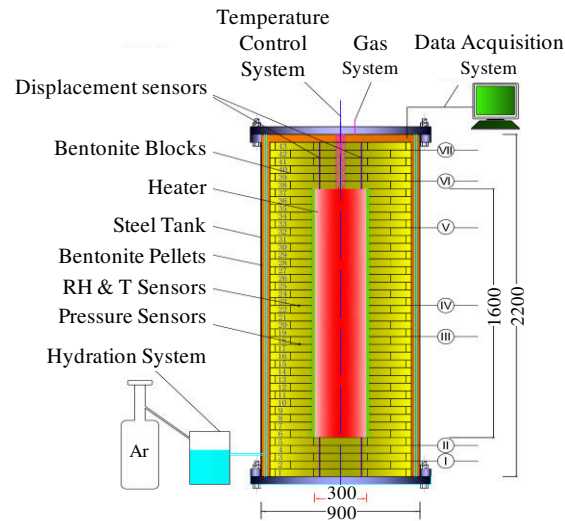


Figure 1. Sketch of the China-Mock-up facility (units: mm).

Table 1. Mineral compositions of GMZ-Na-bentonite (%)

Sample	quartz	feldspar	cristobalite	montmorillonite	kaolinite	calcite
GMZ-001	8.7	7.6	9.0	73.2	0.75	0.75
GMZ-06	8.9	5.8	9.0	74.0	1.53	0.76

The used water of hydration system was sampled at the depth of 524.24 m from borehole BS05 in Beishan site located in northwest China which was currently considered as the most potential site for final disposal in China (Wang 2010). The main chemical compositions are SO_4^{2-} (718mg/L), Cl^- (771mg/L), Na^+ (798mg/L), Ca^{2+} (177mg/L). The swelling property and permeability of bentonite could be influenced by chemical compositions of underground water.

More than 160 sensors were installed within the experiment to measure the important parameters, including the temperature, pore pressure, relative humidity, water injection pressure and total pressure. The sensors are distributed in the seven sections (I~VII) in a vertical direction located in or between the bentonite blocks and pellets. Most of the sensors used were made in China except for the RH sensor (HW4) which was made in Switzerland.

OPERATION OF CHINA-MOCK-UP TEST

The China-Mock-up experiment was assembled completely on 10th September 2010. After a pre-operational phase, the real-time data acquisition and monitoring system have